Marine Pollution Bulletin 194 (2023) 115429

Contents lists available at ScienceDirect

Marine Pollution Bulletin

journal homepage: www.elsevier.com/locate/marpolbul

Distribution of picophytoplankton in the northern slope of the South China Sea under environmental variation induced by a warm eddy

Wenjing Zhang [a,b,e], Chen Zhang [b], Shan Zheng [a], Yunyan Chen [d], Mingliang Zhu [a], Xiaoxia Sun [a,c,e,*]

[a] Jiaozhou Bay National Marine Ecosystem Research Station, Institute of Oceanology, Chinese Academy of Sciences, Qingdao, China
[b] Muping Coastal Environmental Research Station, Yantai Institute of Coastal Zone Research, Chinese Academy of Sciences, Yantai, China
[c] Laboratory for Marine Ecology and Environmental Science, Laoshan Laboratory, Qingdao, China
[d] Qingdao Institute of Bioenergy and Bioprocess Technology, Chinese Academy of Sciences, Qingdao, China
[e] University of Chinese Academy of Sciences, Beijing, China

ARTICLE INFO

Keywords:
Continental slope
Warm eddy
Picophytoplankton
Vertical distribution
South China Sea

ABSTRACT

Mesoscale eddies have been reported to have a substantial impact on the distribution of phytoplankton through the regulation of environmental variables in the open ocean. However, the influence of warm eddies on phytoplankton in continental slopes remains largely unknown. To reveal the impact of mesoscale eddies within slope regions, we conducted a field investigation of picophytoplankton on the northern slope of the South China Sea during an anticyclonic warm eddy propagation. We observed different picophytoplankton distribution patterns. *Synechococcus* dominated the picophytoplankton community in the Kuroshio-affected eddy core rather than the previously reported *Prochlorococcus*, and *Prochlorococcus* dominated outside the eddy in the shelf. In addition, through further vertical study of typical layers, we found that the influence of warm eddy varied in different layers. Analysis of the mechanisms indicated that the distributions were attributed to warm eddy-induced nutrients and light variations and the physical processes in it.

1. Introduction

The continental slope connects the shallow shelf and deep open sea, and it mediates the exchange of heat, salt, materials, and water masses between them (Laruelle et al., 2018; Qiu et al., 2022). The complex topography of continental slopes, including canyons, ridges, troughs, and straits, results in highly variable currents (Igeta et al., 2021; Thompson et al., 2018; Mizobata et al., 2002) and frequent mesoscale eddies (Cheng et al., 2020; Manucharyan and Isachsen, 2019). Mesoscale eddies formed on continental slopes induce variations in ambient flow (Su et al., 2020; Qiu et al., 2019) and modulate the water mass transformation between the shelf water and open sea (Wei and Wang, 2021), which is different from the stable and simple water mass composition in eddies formed in the open ocean (Wang and Stewart, 2020; Zhang et al., 2022). The complex system of eddies in slope regions results in variable marine environments and biological ecosystems (Jakobsson et al., 2012; Bluhm et al., 2020).

Mesoscale eddies are ubiquitous in oceans worldwide. Phytoplankton biomass and composition inside and outside eddies vary owing to physical turbulence or the doming/sinking of the nutricline induced by eddies (Bibby and Moore, 2011; Barlow et al., 2017; Gao et al., 2017). Phytoplankton are primary producers in marine ecosystems and contribute roughly half of the global photosynthetic primary production (Field et al., 1998). They also play crucial roles in biogeochemical cycles, carbon budgets, and climate change (Litchman et al., 2015). Generally, primary and secondary production has been found to increase in cyclonic cold eddies and decrease in anticyclonic warm eddies (Xiu and Chai, 2011; He et al., 2019). However, biological responses to anticyclonic eddies are complex. Some studies have reported positive effects on the phytoplankton abundance in warm eddies. Phytoplankton blooms occur in the center of the South China Sea because of the transport of coastal nutrients by a large warm eddy (Lin et al., 2010). Wang et al. (2018) found enhanced phytoplankton biomass at the edge of a warm eddy, which resulted from a nutrient pump at the edge. In addition, little difference between phytoplankton biomass or Chl a concentration inside and outside warm eddies have been documented in the Pacific Ocean (Dai et al., 2020; Huang et al., 2010; Ning, 2004; Shih et al., 2020) and Atlantic Ocean (Sweeney et al., 2003). Despite the wide

* Corresponding author at: Jiaozhou Bay National Marine Ecosystem Research Station, Institute of Oceanology, Chinese Academy of Sciences, Qingdao, China.
E-mail address: xsun@qdio.ac.cn (X. Sun).

https://doi.org/10.1016/j.marpolbul.2023.115429
Received 24 April 2023; Received in revised form 4 August 2023; Accepted 15 August 2023
Available online 28 August 2023

recognition of the spatial distribution of phytoplankton in the water column inside and outside mesoscale eddies, the influence of different layers has received less attention. And previous studies on the biochemical influences of mesoscale eddies have primarily focused on the open sea or basin scale, and the biological responses to warm eddies on continental slopes, especially phytoplankton abundance and community composition, are less understood. Rodríguez et al. (2003) preliminarily revealed that phytoplankton distributions above 100 m were influenced by an anticyclonic eddy on the slope of Biscay Bay and found a two-fold increase in Chl a concentration at the eddy core relative to that at reference stations. Using satellite and numerical models, Geng et al. (2021) found a phytoplankton bloom on the slope of the South China Sea resulting from the interaction of a mesoscale eddy and river plume. Such limited observations and reports have resulted in uncertainty regarding the biological influences of mesoscale eddies in slope regions.

The South China Sea is the largest semi-enclosed marginal sea in the western Pacific Ocean. The northern slope of the South China Sea, located between the shelf water, which is rich in nutrients and Chl a, and the oligotrophic and open basin area, plays an important role in the material and energy exchange between the shelf water and basin water (Xu et al., 2018). Mesoscale eddies frequently occur in the northern South China Sea (Guo et al., 2017). The intrusion of water from the Kuroshio Current, characterized by high temperature, high salinity, and depleted nutrients from Luzon Island, is a dominant factor in eddy formation in the northern South China Sea, where more anticyclonic warm eddies are shed from the Kuroshio Current Loop in winter and early spring under the influence of the northeasterly monsoon (Nan et al., 2011).

Based on satellite oceanographic sea-level anomaly (SLA) data from AVISO (http://www.aviso.altimetry.fr), an anticyclonic warm eddy propagated southwest along the northern slope of the South China Sea in March 2017. It originated from the Kuroshio Current. A branch of the Kuroshio passed through the Luzon Strait and flowed into the northern slope of the South China Sea. It flowed southwest to the continental shelf and looped together with South China Sea water and shelf water to form the warm eddy (Graphic Abstract, Fig. 1, and Fig. A1). To study the biological effect of warm eddies on continental slopes, we conducted a field investigation during warm eddy movement along a continental slope. The objective of this study was to use picophytoplankton data from flow cytometry (CytoBuoy Inc., Holland, UK) to reveal the three-dimensional structure of picophytoplankton communities inside and outside a warm eddy on a continental slope. In particular, we examined: (1) The horizontal difference in picophytoplankton composition in the water column inside and outside warm eddies; (2) The influence of warm eddies on the vertical distribution of picophytoplankton; (3) The influence of warm eddies on phytoplankton distribution in typical water layers.

2. Materials and methods

2.1. Sample collection

The field investigation was conducted at 16 stations in the northern slope of South China Sea while aboard the research vessel "Nanfeng" from March 17 to 31 in 2017 (Fig. 1). The study area was defined as three groups: eddy core (EC), eddy edge (EE) and out of eddy (OE) based on the closed contour of sea level anomaly. Stations 5, 6, 10, 11, 12, 13, and 14 were located in the EC, and stations 2, 3, 4, 7, and 15 were in the EE, stations 1, 8, 9, and 16 were in the OE. We also clustered the stations according to their temperature, salinity, and density data, and the results were consistent with the defined groups (Fig. A2).

A Sea-Bird 911 CTD (Sea-Bird Scientific Inc., United States) was utilized to record hydrographic data at different depths, including the temperature, salinity and photosynthetically available radiation (PAR) level. Phytoplankton and nutrient levels were determined from seawater samples taken at 5–6 depths (Table 1) up to 200 m below the surface (in some cases the bottom depth was <200 m) using a 10 L Niskin sampler (KC-Denmark Inc., Denmark) bundled with a CTD. The concentrations of ammonia, nitrate, nitrite, and phosphate were measured using an autoanalyzer (Skalar SAN^{plus}). The detectable lines for these nutrients were 0.02 μmol/L, 0.02 μmol/L, 0.01 μmol/L, and 0.01 μmol/L, respectively (Zhang et al., 2012). The phytoplankton samples were fixed with 5 % glutaraldehyde and immediately stored at −80 °C until the estimation by CytoSub.

2.2. Quantifying phytoplankton abundance

Picophytoplankton analyses were conducted using CytoSub flow cytometer software. The fixed phytoplankton samples were thawed at room temperature and scanned using CytoSub for 3 min at a rate of 15 μL/s. Each cell was intercepted by a 15 MW laser beam with a wavelength of 488 nm as it passed through the CytoSub flow cell; the optical pulse shape signals were then recorded. The forward scatter signal was collected using a PIN photodiode as a proxy for cell size. The sideward scatter signal was related to the complexity inside the cells. The fluorescence signals were dispersed via a concave holographic grating and collected using a hybrid photomultiplier. The wavelengths of the red

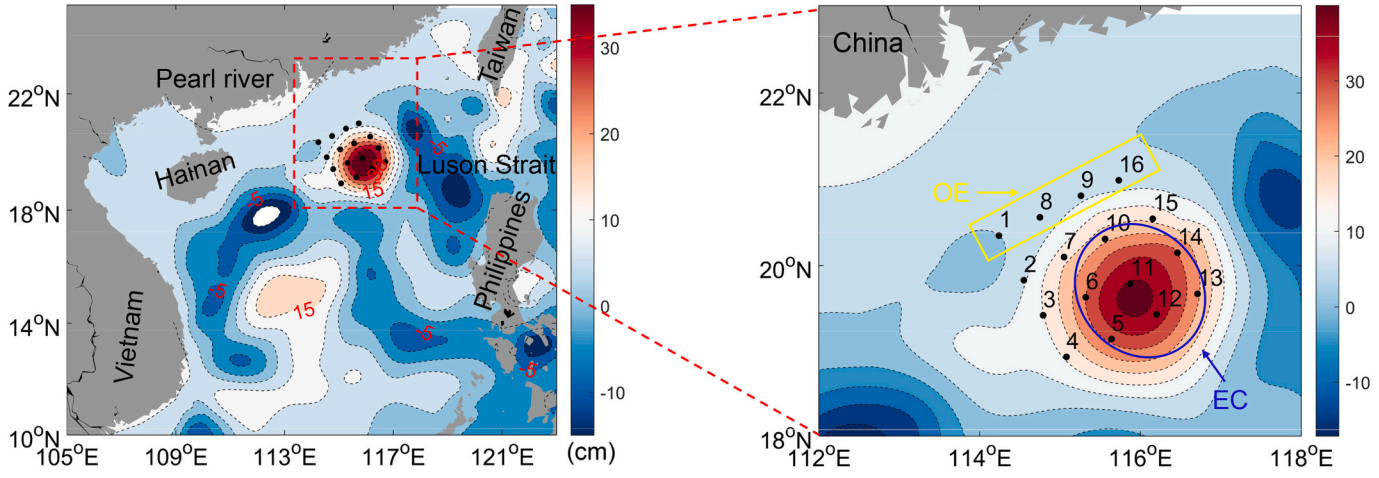

Fig. 1. A map of sea level anomaly (cm) and sampling stations in the study area in March 2017.
Notes: The black points were the sampling stations. The stations in yellow box were not affected by the warm eddy (OE), and in the blue box were located at the eddy core (EC). And the remaining stations were stations at the eddy edge (EE).

Table 1
Sampling information from the stations in the northern South China Sea in March 2017.

Locations	Station	Longitude	Latitude	Bottom depth(m)	Date	Sampling depth (m)
OE	1	114.23	20.33	122	2017.03.17	5,24,40,50,90,115
	8	114.73	20.56	122	2017.03.22	5,25,70,100,121
	9	115.27	20.79	180	2017.03.22	5,40,70,100,175
	16	115.74	21.00	208	2017.03.25	5,25,40,70,100,205
EE	2	114.49	19.87	543	2017.03.17	5,30,60,85,130,200
	3	114.77	19.38	1280	2017.03.19	5,25,50,75,110,200
	4	115.12	18.92	2808	2017.03.19	5,25,60,80,120,200
	7	115.01	20.09	472	2017.03.21	5,15,48,65,105,200
	15	116.12	20.61	514	2017.03.25	5,40,65,100,200
EC	5	115.6	19.17	2700	2017.03.20	5,25,40,80,130
	6	115.33	19.63	2087	2017.03.21	5,25,40,75,140,200
	10	115.6	20.36	518	2017.03.23	5,25,80,160,200
	11	115.87	19.85	1514	2017.03.23	5,25,50,90,120,200
	12	116.18	19.4	1969	2017.03.23	5,25,50,85,120,200
	13	116.75	19.66	2017	2017.03.24	5,25,50,80,120,200
	14	116.39	20.10	993	2017.03.24	5,25,50,85,120,200

fluorescence (FLR), orange fluorescence (FLO), and yellow fluorescence (FLY) signals were 668–734 nm, 601–668 nm, and 536–601 nm, respectively. To capture the optical pulse of the target particles and avoid signals from background noise and non-photosynthetic cells, we set 10 mV as the trigger FLR threshold. Images of each particle were captured as they passed through the flow cell, and the pulse-shape signals, including the forward scatter, were also recorded using CytoSub.

Based on the optical characteristics recorded using CytoSub, the sampled picophytoplankton were classified into three taxa and counted separately: *Prochlorococcus*, *Synechococcus*, and picoeukaryotes (Fig. 2). Beads with a diameter of 1 μm were used as a size reference. *Prochlorococcus* has the minimum size and high FLR which is related to its Chl a content (Chisholm et al., 1988). *Synechococcus* is characterized by a high FLR and FLO (FLO is related to phycoerythrin) (Waterbury et al., 1979). Picoeukaryotes also feature a high FLR, and their size ranges from 1 to 2 μm (Dugenne et al., 2014).

2.3. Data analysis

Phytoplankton data were analyzed using the CytoClu3 software (CytoBuoy). Statistical differences among the phytoplankton abundance and specific depth in OE, EE, and EC samples were determined using the *t*-test, Wilcox test, or ANOVA using R version 4.1. Redundancy Analysis (RDA) was used to identify the environmental variables that regulate phytoplankton distribution, using R version 4.1 (vegan package). Prior to analysis, the phytoplankton and environmental data were transferred using Hellinger and log (X + 1), respectively. Monte Carlo permutations (999 times) were used to select significant driving factors for the RDA model. Distribution data were presented using Surfer 11.0 (Golden Software Inc., Golden, CO, United States), OriginPro 9.0 (OriginLab Co, Massachusetts, United States), and Ocean Data View 5.3.0 (Reiner Schlitzer, Alfred Wegener Institute, Bremerhaven, Germany).

3. Results

3.1. Distribution of environmental variables

The temperature–salinity diagram in Fig. 3 shows the source water types of the South China Sea water, Kuroshio Current, and Shelf water, as well as the CTD data of all the sampling station locations (OE, EE, and EC). The data of the Kuroshio Current water and the South China Sea water were from Argo data from AVISO, and the statistical core salinity and temperature of the Shelf water were cited from Zhu et al. (2019) and Gao et al. (2020). The distributions of nutrients, temperature, and salinity (Fig. 4) were affected by the water masses and physical processes associated with the warm eddy. Influenced by the Kuroshio Current and South China Sea water, nutrients were scarce at the sea surface in OE, EE, and EC, with undetectable nitrite and nitrate levels at each station and average ammonia and phosphate concentrations of 0.04 ± 0.03 μmol/L and 0.02 ± 0.01 μmol/L, respectively. Water was

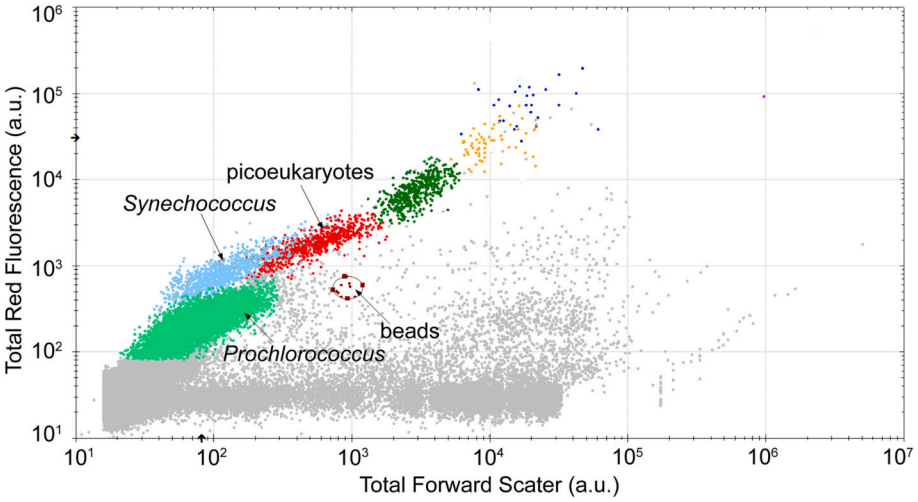

Fig. 2. Phytoplankton classification using CytoClu3
Notes: The grey, cyan, light blue and red dots were background noise, *Prochlorococcus*, *Synecococcus* and picoeukaryotes, respectively. The dots in the red circle were beads with a diameter of 1 μm. (For interpretation of the references to colour in this figure legend, the reader is referred to the web version of this article.)

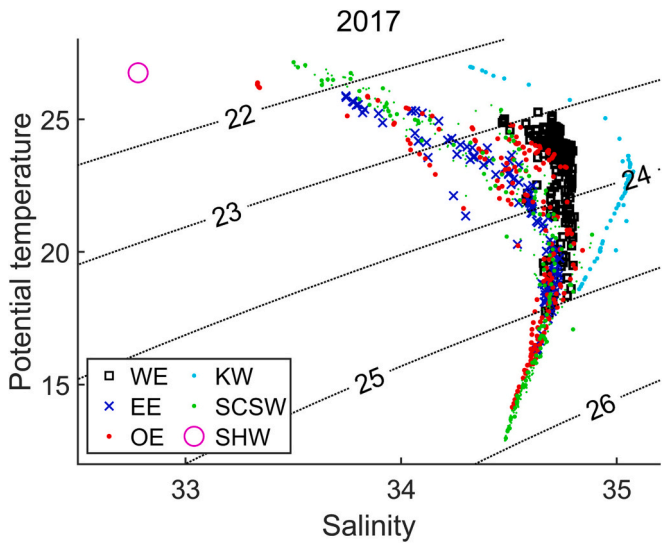

Fig. 3. Temperature–salinity diagram of outside of the eddy (OE), eddy edge (EE), and eddy core (EC) in March 2017
Notes: KW: Kuroshio Current water; SCSW: South China Sea water; SHW: Shelf water.

nitrogen-limited above 100 m, with a nitrogen to phosphate ratio less than the Redfield stoichiometry of 16. Nitrogen was significantly more limited in EE and EC than in OE (ANOVA, $p < 0.05$). The average nitrogen to phosphate ratios were 12.36, 6.18, and 4.67 in OE, EE, and EC, respectively. The concentration of nutrients increased at 200 m; nitrogen-limited conditions were relieved at 100 m in OE and EE and 150 m in EC.

The OE stations were located on the continental shelf, which is characterized by high temperature and low salinity from the surface to 150 m in depth, influenced by a mixture of the Kuroshio Current, the South China Sea, and shelf water. Due to the influence of shelf water, the average nutrient levels above 100 m were higher in OE samples than in EC (*t*-test, $p < 0.05$). The average concentrations of nitrogen and phosphate were 0.68 ± 0.46 μmol/L and 0.11 ± 0.08 μmol/L in OE and 0.05 ± 0.02 μmol/L and 0.03 ± 0.01 μmol/L in EC, respectively.

Water above 100 m at the EC stations was a mixture of the Kuroshio Current (high temperature and salinity) and the South China Sea (low temperature and salinity) water. Nutrients were poor above 100 m at EC stations, influenced by the oligotrophic Kuroshio Current and South China Sea water. The convergence and downwelling at the EC caused the surface water to sink and deepen the isothermal, isohaline, and oligotrophic water layers (Fig. 4).

Water above 120 m at the EE stations was mainly affected by the South China Sea water. And an obvious upwelling was observed in EE (Fig. 4), which might be attributed to the nonlinear Ekman effect or the ageostrophic second circulation (Liu et al., 2017; Mahadevan et al., 2008). The upwelling brought mass nutrients from deep-sea water and increased the levels of nitrate and phosphate in particular (Fig. 4c and f).

The PAR of stations in EE and EC estimated in the daytime were shown in Fig. 5. They decreased sharply with depth, and the value at the depth of 150 m was <1.00. The PAR at the depth of 10 m was 777.57 and 216.13 in EE and EC, respectively. It was much higher in the upper 100 m in EE than that in EC.

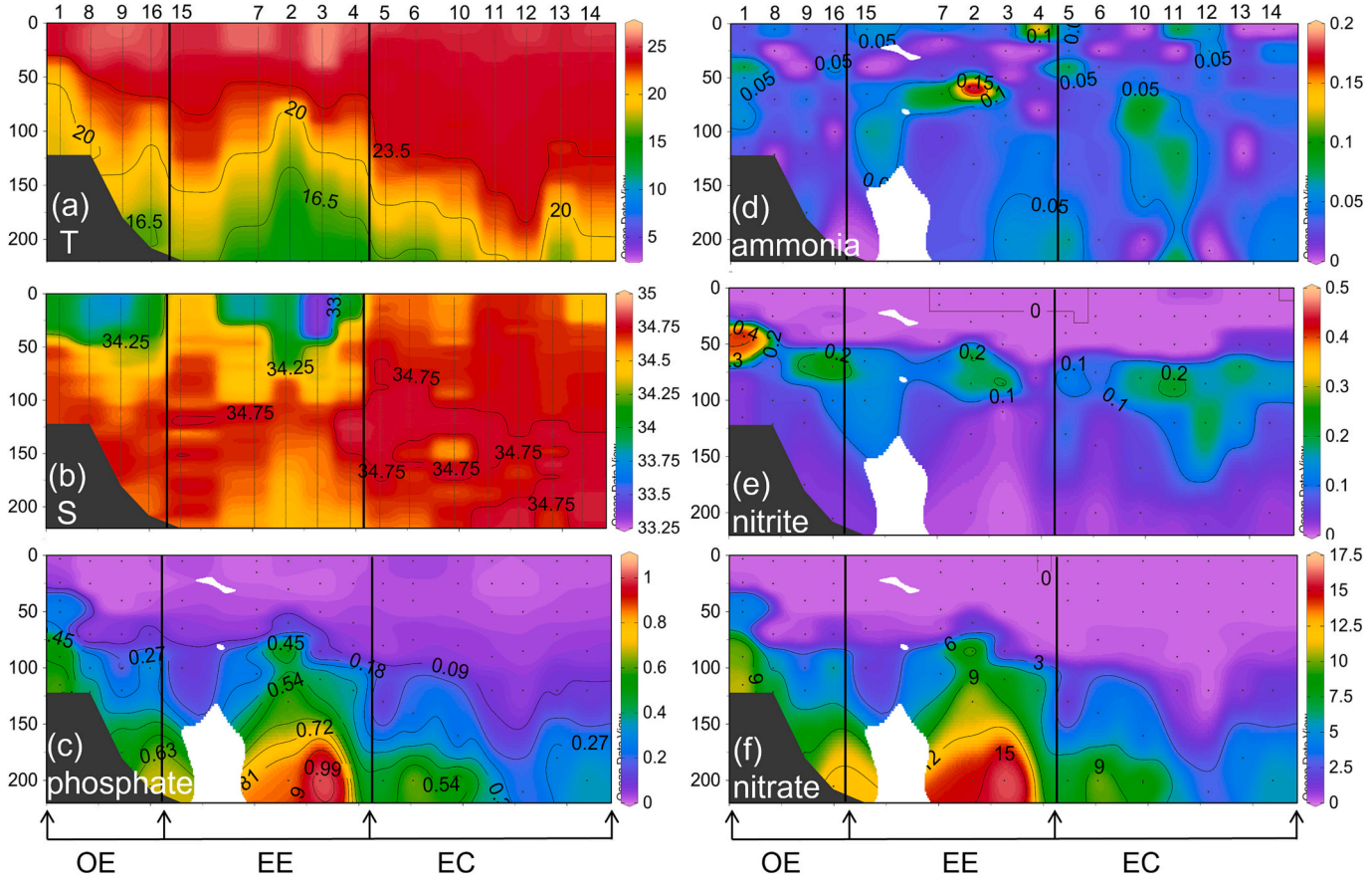

Fig. 4. The distribution of (a) temperature (°C), (b) salinity, (c) phosphate (μmol/L), (d) ammonia (μmol/L), (e) nitrite (μmol/L), and (f) nitrate (μmol/L) in eddy edge (EE), outside of the eddy (OE), and eddy core (EC).

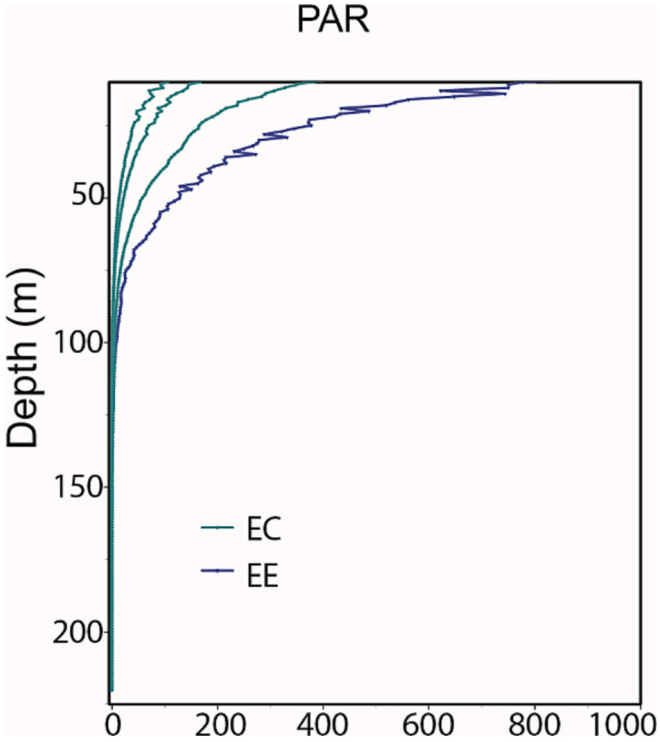

Fig. 5. The distribution of photosynthetically available radiation (PAR) at the eddy core (EC) and the eddy edge (EE) in March 2017.

3.2. Horizontal distribution of picophytoplankton

The average abundance was calculated using the depth-integrated abundance divided by the bottom depth of the stations, or by 200 if the bottom depth was >200 m, to evaluate the horizontal distribution of phytoplankton. The average abundance of picophytoplankton was 14,034.57 ± 5176.19 cells/ml, among which *Synechococcus* and *Prochlorococcus* were responsible for 49.56 % and 44.72 %, respectively. The *Synechococcus* and *Prochlorococcus* concentrations were similar, with averages of 6955.19 ± 4032.90 cells/ml and 6276.22 ± 4085.55 cells/ml, respectively, which were an order of magnitude higher than the concentration of picoeukaryotes (803.16 ± 354.85 cells/ml).

The average picophytoplankton abundance in the OE, EE, and EC samples was 16,833.25 ± 6732.99 cells/ml, 13,334.49 ± 1164.65 cells/ml, and 12,935.39 ± 6030.91 cells/ml, respectively (Fig. 6a). Different picophytoplankton community structures were found in the OE and EC samples; *Prochlorococcus* was the most abundant in OE and accounted for 62.23 % of the total phytoplankton, whereas *Synechococcus* dominated in EC and contributed 63.25 % of the total phytoplankton biomass (Fig. 6b). *Synechococcus* abundance in EC samples (8496.25 ± 4877.94 cells/ml) was 1.68 times higher than that in OE (5064.34 ± 2686.79 cells/ml). The *Prochlorococcus* abundance in OE samples (10,857.18 ± 4742.00 cells/ml) was significantly higher than that in EE (6384.16 ± 2507.10 cells/ml) and EC (3581.43 ± 1955.41 cells/ml) (ANOVA, $p < 0.01$).

3.3. Vertical distribution of picophytoplankton

In general, the phytoplankton abundance first increased and then decreased with increasing depth (Figs. 7 and A3). *Synechococcus* dominated the picophytoplankton community above 25 m in OE, EE, and EC samples (Fig. 7). The composition became distinct in OE, EE, and EC samples at depths below 25 m. In OE samples, the picophytoplankton community was dominated by *Prochlorococcus* below 25 m, with a contribution of up to 90 % at depths of 100 m or greater (Fig. 7b). In EE samples, *Synechococcus* was abundant above 75 m, with a contribution exceeding 50 % (53.10 %–68.8 %), while *Prochlorococcus* was dominant below 75 m, with contributions of 82.66 % at 110 m and 68.88 % at 200 m (Fig. 7d). In EC samples, *Synechococcus* was the most abundant picophytoplankton at the depth above 200 m (the abundance of *Prochlorococcus* was the highest and contributed 65.87 % of the community at 200 m), with contributions ranging from 49.66 % to 85.48 % (Fig. 7f). Vertically, *Prochlorococcus* was dominant from the subsurface to 200 m in depth in OE samples, whereas *Synechococcus* was dominant above 200 m in depth in EC samples.

3.4. Distribution of picophytoplankton in typical layers

To reveal the fine vertical structure influenced by warm eddies, we explored the distribution of picophytoplankton in different layers (Fig. 8). At the sea surface, picophytoplankton abundance was 2920.42 ± 2396.38 cells/ml and 2330.87 ± 1355.06 cells/ml in EE and EC samples, respectively, with no statistical difference ($p > 0.05$). At the depth of abundance maximum (DAM), the abundance of picophytoplankton was significantly higher in EE samples than in EC (*t*-test, $p < 0.05$). This difference was attributed to the concentration of *Prochlorococcus* in EE samples (19,303.09 ± 14,022.35 cells/ml), which was significantly higher than that in EC (7570.04 ± 3161.15 cells/ml) (t-test, $p < 0.05$). The abundance of picoeukaryotes in EE samples was higher than that in EC, with an average of 2915.37 ± 997.45 cells/ml and 2400.38 ± 447.12 cells/ml, respectively. At 200 m, the picophytoplankton abundance was statistically higher in EC samples (906.78 ± 405.64 cells/ml) than in EE (303.93 ± 143.87 cells/ml) (t-test, $p < 0.05$). The abundance of *Synechococcus*, *Prochlorococcus*, and picoeukaryotes was 3.20, 2.85, and 4.03 times higher in EC than in EE.

The DAM of phytoplankton gradually became deeper from the OE stations to the EE and then to the EC, with average depths of 62.50 ± 15.00 m, 69.00 ± 8.22 m, and 72.14 ± 15.77 m, respectively. The DAMs of the different phytoplankton groups were between 55 and 95 m (Fig. A3). For *Synechococcus*, the DAM was 58.50 ± 23.00 m at the OE stations, 69.00 ± 8.22 m at the EE. and 72.14 ± 15.77 m at the EC (Fig. A3b), and the depths at the EE and EC were significantly higher

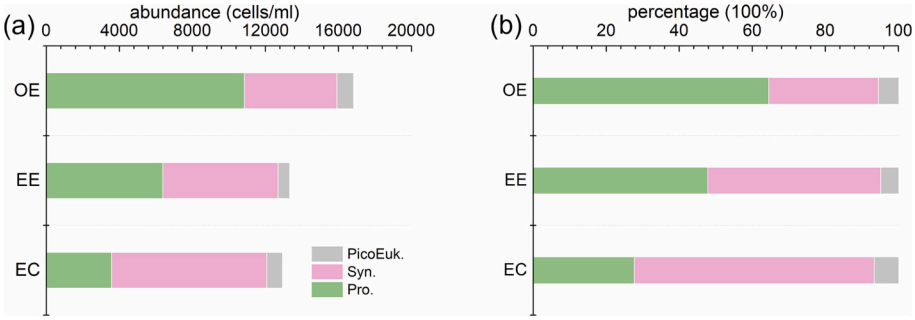

Fig. 6. Average abundance (a) and percentage (b) of *Prochlorococcus*, *Synechococcus*, and picoeukaryotes in epipelagic zones in March 2017.

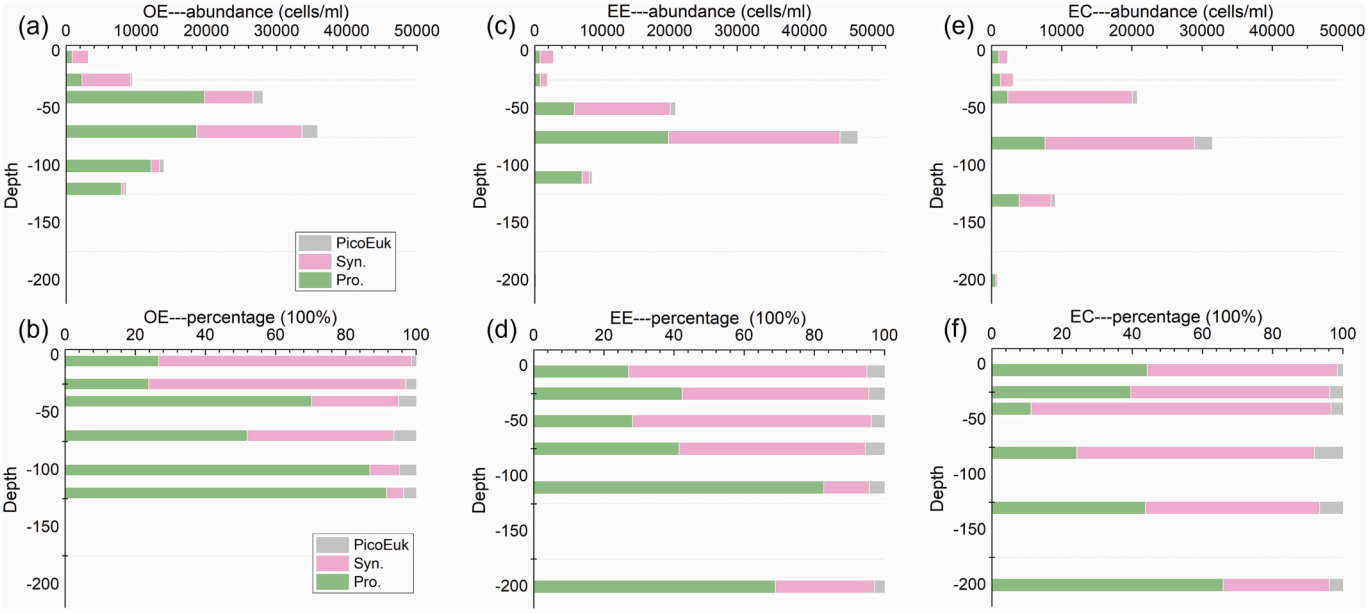

Fig. 7. Depth distribution and percentage of picoplankton group abundance and relative contribution in eddy core (EC) (a, b), eddy edge (EE) (c, d) and outside of the eddy (OE) (e, f).

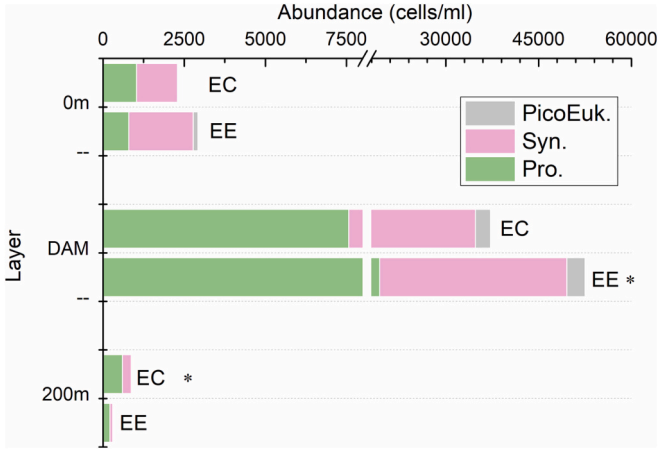

Fig. 8. The distribution of picophytoplankton in the typical layers in eddy edge (EE) and eddy core (EC)
Notes: * meant the picophytoplankton abundance in the group was significantly higher than the other one.

than those at the OE (t-test, $p < 0.05$). For picoeukaryotes, the DAM was 65.00 ± 10.00 m at the OE stations, 69.00 ± 8.22 m at the EE, and 77.14 ± 12.86 m at the EC (Fig. A3d). The DAM for *Prochlorococcus* was deeper than that for *Synechococcus* and picoeukaryotes, at 70.00 ± 24.49 m, 82.00 ± 14.83 m, and 93.57 ± 35.91 m at the OE, EE, and EC stations, respectively (Fig. A3c).

3.5. Relationship between phytoplankton abundance and environmental factors

The RDA tri-plot, including the relationships among the sampling locations, phytoplankton abundance, and environmental variables in EC, EE, and OE samples, is shown in Fig. 9. Nitrate, phosphate, temperature, depth, nitrite, and salinity were selected as variables to account for the picophytoplankton distribution ($p = 0.001$). The first and second axes accounted for 58.38 % and 41.06 % of the picophytoplankton community, respectively. The distribution of stations and environmental variables in the tri-plots showed that the influence of environmental factors on OE, EE, and EC was nonspecific. *Synechococcus* was negatively correlated with depth, salinity, and nutrients, whereas *Prochlorococcus* was positively correlated with nitrate, phosphate, depth, and salinity. Nitrate ($r^2 = 0.62$, $p = 0.001$) and phosphate ($r^2 = 0.53$, $p = 0.001$) were the two most significant factors driving the variation in picophytoplankton. Picoeukaryotes were mainly explained by the second axis and were positively correlated with nitrite.

4. Discussion

4.1. Vertical distribution of picophytoplankton

The *Synechococcus* dominated at the upper 25 m layer, while *Prochlorococcus* was dominant at the subsurface (in OE, Fig. 7b) or even below the depth of the DAM (in EE, Fig. 7d). The DAM of *Prochlorococcus* was also much deeper than that of *Synechococcus*. The distribution pattern was not unusual in marine ecosystems (Belkin et al., 2022; Carvalho et al., 2019; Li et al., 2017). The vertical distributions of *Synechococcus* and *Prochlorococcus* were strongly associated with light intensity (Flombaum et al., 2013, 2020), which was attributed to the preference for a well-lit environment by *Synechococcus* and low-lit water by *Prochlorococcus*. In this study, the PAR decreased sharply with depth (Fig. 5), and the light intensity in deeper water was more suitable for the growth of *Prochlorococcus*. The RDA results also showed that *Prochlorococcus* abundance was positively correlated with depth, whereas *Synechococcus* abundance was negatively correlated with depth.

4.2. Distribution of Synechococcus and Prochlorococcus influenced by the warm eddy

The distribution of picophytoplankton in the South China Sea had been widely investigated that the *Synechococcus* was the most abundant in continental shelf, while *Prochlorococcus* was the most abundant in the continental slope (Cai et al., 2007; Chen et al., 2011). Besides, it has been reported that *Prochlorococcus* prefers oligotrophic warm eddies (Belkin et al., 2022; Carvalho et al., 2019; Li et al., 2017) and was considered as the bioindicator of the Kuroshio Current (Huang et al., 2019; Zhao et al., 2019), meanwhile the abundance of *Synechococcus* in warm eddies was significantly lower than that of *Prochlorococcus*

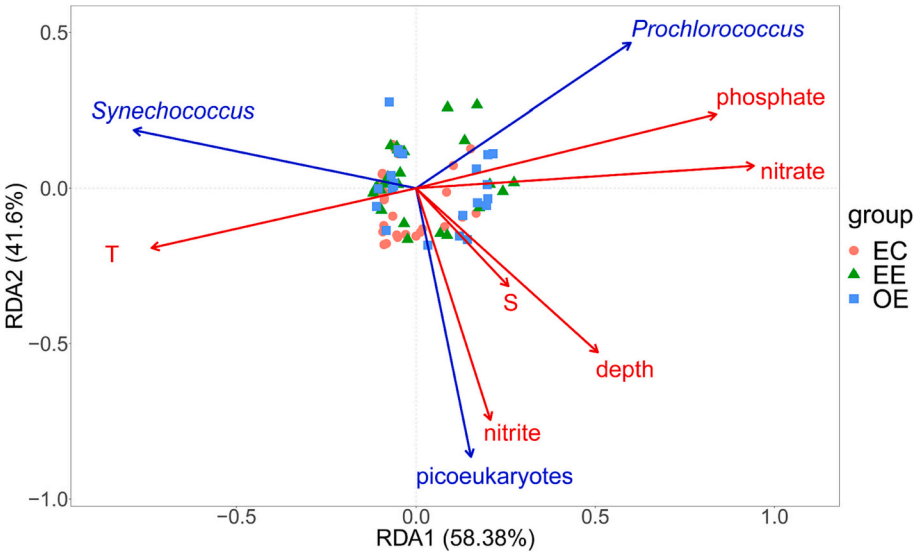

Fig. 9. The redundancy analysis (RDA) between the abundance of picophytoplankton and environmental factors in March 2017.

(Carvalho et al., 2019; Wang et al., 2018). However, the distribution in our study was not consistent with the reported distributional pattern of *Prochlorococcus* and *Synechococcus* under the influence of the warm eddy in the continental slope region. In our study, *Prochlorococcus* dominated in the OE samples in the continental shelf rather than in the Kuroshio Current-affected warm eddy, where was dominated by *Synechococcus* regardless of the water column or depth (Fig. 6b, Fig. 7f). This finding aligns with the results of Dai et al. (2020), who analyzed the phytoplankton community structure in the same cruise through the evaluation of pigments using HPLC-CHEMTAX techniques.

RDA tri-plot showed eddy-induced nutrients variation played a pivotal role in the distribution of the *Synechococcus*, *Prochlorococcus* and picoeukaryotes in the northern slope of the South China Sea. Influenced by the mixture of the Kuroshio current and the South China Sea water, it was oligotrophic and nitrogen-limited in the upper water inside and outside of the eddy during the cruise (Fig. 4 c-f). The downwelling at the warm eddy deepen the nutrient-depleted surface water and decreased the nutrients in EC and EE. Meanwhile the shelf water at OE stations facilitated higher nutrients concentration in OE than EC and EE.

Prochlorococcus and *Synechococcus* were highly competitive in nutrient-limited water (Tsiola et al., 2016), and *Prochlorococcus* would outgrow *Synechococcus* under nitrogen limitation when heterotrophic bacteria existed (Calfee et al., 2022). Although we did not sample heterotrophic bacteria, they did exist in global seawater. Therefore, *Prochlorococcus* was more abundant than *Synechococcus* under nitrogen-limited conditions in OE samples. Besides, phosphate also affects the growth of *Prochlorococcus* and *Synechococcus*. Zubkov et al. (2007) found that *Prochlorococcus* contributed to an average of 45 % of the phosphate uptake, whereas *Synechococcus* was only responsible for 7 % in nutrient-depleted oceans. Thus, *Prochlorococcus* required more phosphate than *Synechococcus*, and higher phosphate concentration at OE locations facilitated the growth of *Prochlorococcus*. RDA analysis showed phosphate concentration positively correlated with the *Prochlorococcus* abundance and negatively correlated with the *Synechococcus*, which also indicated that phosphate was not the limiting factor for the growth of *Synechococcus*. Furthermore, the increase in phosphate could likely stimulated the abundance of *Prochlorococcus* at the EC locations.

Synechococcus is found specifically responding to nanomolar concentrations of nitrate under nitrogen-depleted conditions (Domínguez-Martín et al., 2022). This evolutionary feature facilitates *Synechococcus* outcompeting *Prochlorococcus* in natural marine environments. This may explain the dominance of *Synechococcus* in the nutrient-depleted EC samples in our study. The low nutrient concentration in EC samples was even lower than that in the main Kuroshio Current branch after it mixed with South China Sea water at the EC stations. In the main Kuroshio Current branch near Luzon Strait, the annual sea surface nitrate and phosphate concentration was 0.2 μmol/L and 0.14 μmol/L, respectively (Li et al., 2010). The concentration of nutrients gradually decreased from winter to spring and spring to summer, and the average surface concentration of nitrate plus nitrite was 0.11 ± 0.84 μmol/L in winter (December) and 0.03 ± 0.12 μmol/L in spring (late April–May) (Lee Chen et al., 2008) in the main Kuroshio Current branch. At the EC stations on the slope of the South China Sea, the ammonia concentration in some layers within 200 m and the nitrate and nitrate concentrations in the upper 100 m were undetectable (Fig. 4); the average surface concentration of nitrate plus nitrite was 0.02 ± 0.03 μmol/L in early spring of the study period. Under these conditions, *Synechococcus* can grow well, depending on its ability to assimilate nanomolar concentrations of nitrate at EC locations. The negative relationship between nutrients and *Synechococcus* abundance also verified that nutrients were not a limiting factor for growth.

Above all, the eddy-induced different mixing of water mass and the further redistribution of nutrients inside and outside of the warm eddy led to the interesting distribution pattern of *Prochlorococcus* and *Synechococcus* inner and outer the eddy.

4.3. *The influence of the warm eddy on the distribution of picophytoplankton in different layers*

We analyzed the distribution of picophytoplankton in different layers, and a distinct distribution of picophytoplankton influenced by warm eddies in the typical layers was observed. There was no difference in the abundances in EE and EC samples taken at the sea surface; at the DAM, the abundance of picophytoplankton was the highest in EE samples; at 200 m, the abundance in EC samples was significantly higher than that in EE (Fig. 8).

At the sea surface, similar water masses (Kuroshio Current and South China Sea water) resulted in similar temperatures and nutrient levels at both EC and EE stations (Figs. 3 and 4), and thus similar picophytoplankton abundances. Wang et al. (2018) also reported similar phytoplankton composition across three anticyclonic eddies and attributed this to their similar origins and stages.

At the DAM, the nutrient concentration increased in EE due to the upwelling (Fig. 4), but still limited the growth of phytoplankton. *Prochlorococcus* and picoeukaryotes were positively correlated with nutrient levels (Fig. 9). When the nutrient concentration was <1 μmol/L

nitrate + nitrite, the proportion of picophytoplankton increased (Agawin et al., 2000). The nitrogen concentration at the DAM was 0.83 ± 0.80 μmol/L in EE samples and 0.30 ± 0.20 μmol/L in EC, so the nutrients level in EE samples was more favorable for the growth of picophytoplankton than that in EC. Thus, higher total picophytoplankton concentrations were found in EE samples at the DAM. Furthermore, the light irradiance was more weakened in the EC than EE stations due to the downwelling (Cornec et al., 2021). In this study, the PAR at the depth of DAM was 27.23 and 6.36 in EE and EC, respectively. The light at EE locations was more beneficial for phytoplankton than that at EC. Therefore, both nutrient and light variation induced by the physical processes in EE and EC at the DAM resulted in the enhancement of picophytoplankton in EE locations.

At 200 m, the nutrient concentration increased significantly, with the nitrate concentration reaching 7.23 ± 2.89 μmol/L and 12.24 ± 5.66 μmol/L in EC and EE samples, respectively, which could satisfy the growth requirements of picophytoplankton (Agawin et al., 2000). In addition, light intensity decreases with depth, and the PAR at the depth of 200 m was only 0.12, which was <0.05 % of the surface light (Fig. 5). The light irradiance was also insufficient for phytoplankton at 200 m. Considering that there were few differences in both nutrients and light at the EE and EC stations, mesoscale physical processes were likely responsible for the high phytoplankton biomass in at the EC. The downwelling at the EC stations deepened the mixed layer, the isotherm of 20 °C sank at 188.14 ± 24.11 m, and the isohaline of 34.75-salinity occurred even below 200 m (Fig. 4a and b). The downward sinking of phytoplankton from the upper waters to 200 m also led to the enhancement of phytoplankton at the EC stations at 200 m. The distribution of picophytoplankton also showed a downward spread at EC stations (Fig. A4).

To sum up, the different influences of warm eddy on the distribution of picophytoplankton in typical layers were attributed to the warm eddy-induced nutrients and light intensity variation and the physical processes in the eddy.

5. Conclusions

An anticyclonic eddy along with the intrusion of Kuroshio Current water from the Luzon Strait propagated along the northern slope of the South China Sea in March 2017. During this period, we conducted a field investigation to demonstrate the influence of the warm eddy in the slope area on the distribution of picophytoplankton. The sampling stations were divided into OE, EE, and EC three groups based on the closed contour of the SLA. The distribution of picophytoplankton was different with the reported distribution in continental shelf and slope and inside and outside of the warm eddy. *Synechococcus* was dominant in EC samples rather than at OE stations in the continental shelf, while *Prochlorococcus* was dominant in OE rather than at Kuroshio-affected EC stations. These were attributed to the warm eddy-induced water mass mixing and the physical processes inside the eddy redistributing the nutrients. In addition, the influence of the warm eddy differed by water layer. There was no difference in the picophytoplankton abundances in the OE, EE, and EC samples at the sea surface; at the DAM, the abundance of picophytoplankton was the highest in the EE samples; and at 200 m, the abundance in the EC samples was significantly higher than that in the EE. The distinct influences in the typical layers were because the physical processes in the warm eddy redistributed the nutrients and light intensity, and the downwelling in EC enhanced the picophytoplankton sinking at 200 m. This study shed light on the vertically fine distribution of picophytoplankton influenced by mesoscale eddies for the first time, and provided new insights into the biological response to mesoscale eddies in continental slope regions. More studies are needed for the understanding of biological influences of mesoscale eddies in slope regions and if the influences have universal applicability.

CRediT authorship contribution statement

WZ analyzed the raw data and drafted the manuscript. CZ analyzed the hydrological data and physical processes of the work, drafted part of the manuscript, and revised the manuscript. SZ conceived and coordinated the work. YC performed the measurement and classification of the phytoplankton samples. MZ carried out the sample collection. XS managed and coordinated the project, and revised the manuscript. All authors contributed to the article and approved the submitted version.

Funding

This study was supported by International Science Partnership Program of the Chinese Academy of Sciences (Grant No. 133137KYSB20200002), International Mega-Science Project Cultivation Program (Grant No. 121311KYSB20190029-3), Strategic Priority Research Program of the Chinese Academy of Sciences (Grant No. XDB42030402), the Natural Basic Research Program of China (Grant No. 2014CB441504).

Declaration of competing interest

The authors declare that they have no known competing financial interests or personal relationships that could have appeared to influence the work reported in this paper.

Data availability

Data will be made available on request.

Acknowledgments

The authors are grateful the crew of the R.V. Nanfeng for helping during the cruise. We thank the AVISO data project and Dr. Xu and Dr. Liu for providing the marine hydrology and nutrient data.

Appendix A. Supplementary data

Supplementary data to this article can be found online at https://doi.org/10.1016/j.marpolbul.2023.115429.

References

Agawin, N.S.R., Duarte, C.M., Agustí, S., 2000. Nutrient and temperature control of the contribution of picoplankton to phytoplankton biomass and production. Limnol. Oceanogr. 45, 591–600. https://doi.org/10.4319/lo.2000.45.3.0591.

Barlow, R., Lamont, T., Gibberd, M.J., Airs, R., Jacobs, L., Britz, K., 2017. Phytoplankton communities and acclimation in a cyclonic eddy in the southwest Indian Ocean. Deep-Sea Res. I 124, 18–30. https://doi.org/10.1016/j.dsr.2017.03.013.

Belkin, N., Guy-Haim, T., Rubin-Blum, M., Lazar, A., Sisma-Ventura, G., Kiko, R., Morov, A.R., Ozer, T., Gertman, I., Herut, B., Rahav, E., 2022. Influence of cyclonic and anticyclonic eddies on plankton in the southeastern Mediterranean Sea during late summertime. Ocean Sci. 18 (3), 693–715. https://doi.org/10.5194/os-18-693-2022.

Bibby, T.S., Moore, C.M., 2011. Silicate:nitrate ratios of upwelled waters control the phytoplankton community sustained by mesoscale eddies in sub-tropical North Atlantic and Pacific. Biogeosci. 8, 657–666. https://doi.org/10.5194/bg-8-657-2011.

Bluhm, B.A., Janout, M.A., Danielson, S.L., Ellingsen, I., Gavrilo, M., Grebmeier, J.M., Hopcroft, R.R., Iken, K.B., Ingvaldsen, R.B., Jørgensen, L.L., Kosobokova, K.N., Kwok, R., Polyakov, I.V., Renaud, P.E., Carmack, E.C., 2020. The Pan-Arctic continental slope: sharp gradients of physical processes affect pelagic and benthic ecosystems. Front. Mar. Sci. 7.

Cai, Y.M., Ning, X.R., Liu, C.G., Hao, Q., 2007. Distribution pattern of photosynthetic picoplankton and heterotrophic bacteria in the northern South China Sea. J. Integr. Plant Biol. 49 (3), 282–298. https://doi.org/10.1111/j.1744-7909.2007.00347.x.

Calfee, B.C., Glasgo, L.D., Zinser, E.R., 2022. Prochlorococcus exudate stimulates heterotrophic bacterial competition with rival phytoplankton for available nitrogen. mBio. 13 (1), e02571-02521 https://doi.org/10.1128/mbio.02571-21.

Carvalho, A.C.O., Mendes, C.R.B., Kerr, R., Azevedo, J.L.L., Galdino, F., Tavano, V.M., 2019. The impact of mesoscale eddies on the phytoplankton community in the South Atlantic Ocean: HPLC-CHEMTAX approach. Mar. Environ. Res. 144, 154–165.

Chen, B., Wang, L., Song, S., Huang, B., Sun, J., Liu, H., 2011. Comparisons of picophytoplankton abundance, size, and fluorescence between summer and winter in northern South China Sea. Cont. Shelf Res. 31 (14), 1527–1540. https://doi.org/10.1016/j.csr.2011.06.018.

Cheng, Z., Zhou, M., Zhong, Y., Zhang, Z., Liu, H., Zhou, L., 2020. Statistical characteristics of mesoscale eddies on the continental slope in the northern South China Sea. Acta Oceanol. Sin. 39 (3), 36–44.

Chisholm, S.W., Olson, R.J., Zettler, E.R., Goericke, R., Waterbury, J.B., Welschmeyer, N. A., 1988. A novel free-living prochlorophyte abundant in the oceanic euphotic zone. Nature. 334, 340–343.

Cornec, M., Laxenaire, R., Speich, S., Claustre, H., 2021. Impact of mesoscale eddies on deep chlorophyll maxima. Geophys. Res. Lett. 48 (15), e2021GL093470 https://doi.org/10.1029/2021GL093470.

Dai, S., Zhao, Y., Liu, H., Hu, Z., Zheng, S., Zhu, M., Guo, S., Sun, X., 2020. The effects of a warm-core eddy on chlorophyll a distribution and phytoplankton community structure in the northern South China Sea in spring 2017. J. Mar. Syst. 210, 103396 https://doi.org/10.1016/j.jmarsys.2020.103396.

Domínguez-Martín, M.A., López-Lozano, A., Melero-Rubio, Y., Gómez-Baena, G., Jiménez-Estrada, J.A., Kukil, K., Diez, J., García-Fernández, J.M., 2022. Marine *Synechococcus* sp. strain WH7803 shows specific adaptative responses to assimilate nanomolar concentrations of nitrate. Microbiol. Spectr. 10 (4), e00187-00122 https://doi.org/10.1128/spectrum.00187-22.

Dugenne, M., Thyssen, M., Nerini, D., Mante, C., Poggiale, J.C., Garcia, N., Garcia, F., Gregori, G.J., 2014. Consequence of a sudden wind event on the dynamics of a coastal phytoplankton community: an insight into specific population growth rates using a single cell high frequency approach. Front. Microbiol. 5, 485. https://doi.org/10.3389/fmicb.2014.00485.

Field, C.B., Behrenfeld, M.J., Randerson, J.T., Falkowski, P., 1998. Primary production of the biosphere: integrating terrestrial and oceanic components. Science. 281 (5374), 237–240.

Flombaum, P., Gallegos, J.L., Gordillo, R.A., Rincon, J., Zabala, L.L., Jiao, N., Karl, D.M., Li, W.K.W., Lomas, M.W., Veneziano, D., Vera, C.S., Vrugt, J.A., Martiny, A.C., 2013. Present and future global distributions of the marine Cyanobacteria Prochlorococcus and Synechococcus. Proc. Natl. Acad. Sci. U. S. A. 110 (24), 9824–9829. https://doi.org/10.1073/pnas.1307701110.

Flombaum, P., Wang, W.L., Primeau, F.W., Martiny, A.C., 2020. Global picophytoplankton niche partitioning predicts overall positive response to ocean warming. Nat. Geosci. 13 (2), 116–120.

Gao, W., Wang, Z., Zhang, K., 2017. Controlling effects of mesoscale eddies on thermohaline structure and in situ chlorophyll distribution in the western North Pacific. J. Mar. Syst. 175, 24–35. https://doi.org/10.1016/j.jmarsys.2017.07.002.

Gao, Y., Huang, R.X., Zhu, J., Huang, Y.X., Hu, J.Y., 2020. Using the sigma-pi diagram to analyze water masses in the northern South China Sea in spring. J. Geophys. Res. Oceans 125, e2019JC015676. https://doi.org/10.1029/2019JC015676.

Geng, B., Xiu, P., Liu, N., He, X., Chai, F., 2021. Biological response to the interaction of a mesoscale Eddy and the River Plume in the Northern South China Sea. J. Geophys. Res. Oceans 126 (9).

Guo, M., Xiu, P., Li, S., Chai, F., Xue, H., Zhou, K., Dai, M., 2017. Seasonal variability and mechanisms regulating chlorophyll distribution in mesoscale eddies in the South China Sea. J. Geophys. Res. Oceans 122 (7), 5329–5347. https://doi.org/10.1002/2016jc012670.

He, Q., Zhan, H., Xu, J., Cai, S., Zhan, W., Zhou, L., Zha, G., 2019. Eddy-induced chlorophyll anomalies in the Western South China Sea. J. Geophys. Res. Oceans 124, 9487–9506.

Huang, B., Hu, J., Xu, H., Cao, Z., Wang, D., 2010. Phytoplankton community at warm eddies in the northern South China Sea in winter 2003/2004. Deep-Sea Res. II 57, 1792–1798. https://doi.org/10.1016/j.dsr2.2010.04.005.

Huang, Y., Laws, E., Chen, B., Huang, B., 2019. Stimulation of heterotrophic and autotrophic metabolism in the mixing zone of the Kuroshio Current and Northern South China Sea: implications for export production. J. Geophys. Res. Biogeosci. 124 (9), 2645–2661. https://doi.org/10.1029/2018jg004833.

Igeta, Y., Kuga, M., Yankovsky, A., Wagawa, T., Fukudome, K., Kaneda, A., Ikeda, S., Tsuji, T., Hirose, N., 2021. Effect of a current trapped by a continental slope on the pathway of a coastal current crossing Toyama Trough. Japan. J. Oceanogr. 77 (4), 685–701.

Jakobsson, M., Mayer, L., Coakley, B., Dowdeswell, J.A., Forbes, S., Fridman, B., Hodnesdal, H., Noormets, R., Pedersen, R., Rebesco, M., Schenke, H.W., Zarayskaya, Y., Accettella, D., Armstrong, A., Anderson, R.M., Bienhoff, P., Camerlenghi, A., Church, I., Edwards, M., Gardner, J.V., Hall, J.K., Hell, B., Hestvik, O., Kristoffersen, Y., Marcussen, C., Mohammad, R., Mosher, D., Nghiem, S. V., Pedrosa, M.T., Travaglini, P.G., Weatherall, P., 2012. The international bathymetric chart of the Arctic Ocean (IBCAO) version 3.0. Geophys. Res. Lett. 39, L12609.

Laruelle, G.G., Cai, W.J., Hu, X., Gruber, N., Mackenzie, F.T., Regnier, P., 2018. Continental shelves as a variable but increasing global sink for atmospheric carbon dioxide. Nat. Commun. 9 (1), 454.

Lee Chen, Y.L., Chen, H.Y., Tuo, S.H., Ohki, K., 2008. Seasonal dynamics of new production from Trichodesmium N2 fixation and nitrate uptake in the upstream Kuroshio and South China Sea basin. Limnol. Oceanogr. 53 (5), 1705–1721.

Li, T., Zhao, J., Sun, R., Chang, F., Sun, H., 2010. The variation of upper ocean structure and paleoproductivity in the Kuroshio source region during the last 200kyr. Mar. Micropaleontol. 75 (1–4), 50–61.

Li, J., Jiang, X., Li, G., Jing, Z., Zhou, L., Ke, Z., Tan, Y., 2017. Distribution of picoplankton in the northeastern South China Sea with special reference to the effects of the Kuroshio intrusion and the associated mesoscale eddies. Sci. Total Environ. 589, 1–10. https://doi.org/10.1016/j.scitotenv.2017.02.208.

Lin, I.I., Lien, C.C., Wu, C.R., Wong, G.T.F., Huang, C.W., Chiang, T.L., 2010. Enhanced primary production in the oligotrophic South China Sea by eddy injection in spring. Geophys. Res. Lett. 37, L16602. https://doi.org/10.1029/2010GL043872.

Litchman, E., Edwards, K.F., Klausmeier, C.A., 2015. Microbial resource utilization traits and trade-offs: implications for community structure, functioning, and biogeochemical impacts at present and in the future. Front. Microbiol. 6.

Liu, F., Tang, S., Huang, R.X., Yin, K., 2017. The asymmetric distribution of phytoplankton in anticyclonic eddies in the western South China Sea. Deep-Sea Res. Part I 120, 29–38. https://doi.org/10.1016/j.dsr.2016.12.010.

Mahadevan, A., Thomas, L.N., Tandon, A., 2008. Comment on "Eddy/Wind Interactions stimulate extraordinary mid-ocean plankton blooms". Science. 320 (5875), 448. https://doi.org/10.1126/science.1152111.

Manucharyan, G.E., Isachsen, P.E., 2019. Critical role of continental slopes in halocline and Eddy dynamics of the Ekman-Driven Beaufort Gyre. J. Geophys. Res. Oceans 124 (4), 2679–2696.

Mizobata, K., Saitoh, S.I., Shiomoto, A., Miyamura, T., Shiga, N., Imai, K., et al., 2002. Bering Sea cyclonic and anticyclonic eddies observed during summer 2000 and 2001. Prog. Oceanogr. 55, 65–75.

Nan, F., Xue, H., Xiu, P., Chai, F., Shi, M., Guo, P., 2011. Oceanic eddy formation and propagation southwest of Taiwan. J. Geophys. Res. 116 (C12) https://doi.org/10.1029/2011jc007386.

Ning, X., 2004. Physical-biological oceanographic coupling influencing phytoplankton and primary production in the South China Sea. J. Geophys. Res. 109 (C10) https://doi.org/10.1029/2004jc002365.

Qiu, C., Mao, H., Liu, H., Xie, Q., Yu, J., Su, D., Ouyang, J., Lian, S., 2019. Deformation of a warm Eddy in the northern South China Sea. J. Geophys. Res. Oceans 124 (8), 5551–5564.

Qiu, C., Yi, Z., Su, D., Wu, Z., Liu, H., Lin, P., He, Y., Wang, D., 2022. Cross-slope heat and salt transport induced by slope intrusion Eddy's horizontal asymmetry in the northern South China Sea. J. Geophys. Res. Oceans 127 (9).

Rodríguez, F., Varela, M., Fernández, E., Zapata, M., 2003. Phytoplankton and pigment distributions in an anticyclonic slope water oceanic eddy (SWODDY) in the southern Bay of Biscay. Mar. Biol. 143 (5), 995–1011.

Shih, Y.Y., Hung, C.C., Tuo, S.h., Shao, H.J., Chow, C.H., Muller, F.L.L., Cai, Y.H., 2020. The impact of eddies on nutrient supply, diatom biomass and carbon export in the Northern South China Sea. Front. Earth Sci. 8, 537332 https://doi.org/10.3389/feart.2020.537332.

Su, D., Lin, P., Mao, H., Wu, J., Liu, H., Cui, Y., Qiu, C., 2020. Features of slope intrusion mesoscale eddies in the Northern South China Sea. J. Geophys. Res. Oceans 125 (2).

Sweeney, E.N., McGillicuddy, D.J., Buesseler, K.O., 2003. Biogeochemical impacts due to mesoscale eddy activity in the Sargasso Sea as measured at the Bermuda Atlantic Time-series Study (BATS). Deep-Sea Res. II 50, 3017–3039. https://doi.org/10.1016/j.dsr2.2003.07.008.

Thompson, A.F., Stewart, A.L., Spence, P., Heywood, K.J., 2018. The Antarctic slope current in a changing climate. Rev. Geophys. 56 (4), 741–770.

Tsiola, A., Pitta, P., Fodelianakis, S., Pete, R., Magiopoulos, I., Mara, P., Psarra, S., Tanaka, T., Mostajir, B., 2016. Nutrient limitation in surface waters of the oligotrophic eastern Mediterranean Sea: an enrichment microcosm experiment. Microb. Ecol. 71, 575–588. https://doi.org/10.1007/s00248-015-0713-5.

Wang, Y., Stewart, A.L., 2020. Scalings for eddy buoyancy transfer across continental slopes under retrograde winds. Ocean Model 147.

Wang, L., Huang, B., Laws, E.A., Zhou, K., Liu, X., Xie, Y., Dai, M.H., 2018. Anticyclonic Eddy edge effects on phytoplankton communities and particle export in the northern South China Sea. J. Geophys. Res. Oceans 123, 7632–7650.

Waterbury, J.B., Watson, S.W., Guillard, R.R.L., Brand, L.E., 1979. Widespread occurrence of a unicellular, marine, planktonic cyanobacteria. Nature. 277, 293–294.

Wei, H., Wang, Y., 2021. Full-depth scalings for isopycnal Eddy mixing across continental slopes under upwelling-favorable winds. J. Adv. Model. Earth Syst. 13 (6).

Xiu, P., Chai, F., 2011. Modeled biogeochemical responses to mesoscale eddies in the South China Sea. J. Geophys. Res. 116, C10006. https://doi.org/10.1029/2010JC006800.

Xu, M.N., Zhang, W., Zhu, Y., Liu, L., Zheng, Z., Wan, X.S., Qian, W., Dai, M., Gan, J., Hutchins, D., A., Kao, S. J., 2018. Enhanced ammonia oxidation caused by lateral Kuroshio intrusion in the boundary zone of the Northern South China Sea. Geophys. Res. Lett. 45 (13), 6585–6593. https://doi.org/10.1029/2018gl077896.

Zhang, G., Zhao, Z., Liu, C., Liu, Q., Ren, J., 2012. Influence of a flood event on salinity and nutrients in the Changshan Archipelago area (Northern Yellow Sea). J. Ocean Univ. China 11, 419–426.

Zhang, L., Liu, C., Sun, W., Wang, Z., Liang, X., Li, X., Cheng, C., 2022. Modeling mesoscale eddies generated over the continental slope, East Antarctica. Front. Earth Sci. 10.

Zhao, Y., Yu, R.C., Kong, F.Z., Wei, C.J., Liu, Z., Geng, H.X., Dai, L., Zhou, Z.X., Zhang, Q. C., Zhou, M.J., 2019. Distribution patterns of picosized and nanosized phytoplankton assemblages in the East China Sea and the Yellow Sea: implications on the impacts of Kuroshio intrusion. J. Geophys. Res. Oceans 124, 1262–1276. https://doi.org/10.1029/2018JC014681.

Zhu, J., Zheng, Q.A., Hu, J.Y., Lin, H.Y., Chen, D.W., Chen, Z.Z., Sun, Z.Y., Li, L.Y., Kong, H., 2019. Classification and 3-d distribution of upper layer water masses in the northern South China Sea. Acta Oceanol. Sin. 38 (4), 126–135. https://doi.org/10.1007/s13131-019-1418-2.

Zubkov, M.V., Mary, I., Woodward, E.M., Warwick, P.E., Fuchs, B.M., Scanlan, D.J., Burkill, P.H., 2007. Microbial control of phosphate in the nutrient-depleted North Atlantic subtropical gyre. Environ. Microbiol. 9 (8), 2079–2089. https://doi.org/10.1111/j.1462-2920.2007.01324.x.